

Pricing discounted American capped options

Tsvetelin S. Zaeveski

Institute of Mathematics and Informatics, Bulgarian Academy of Sciences, Bulgaria

ARTICLE INFO

Article history:

Received 20 April 2021

Revised 20 December 2021

Accepted 20 January 2022

JEL classification:

C41

G12

G13

MSC:

35R35

35Q91

60G44

91G20

Keywords:

American capped options

Optimal boundary

Optimal stopping time

Crank-Nicolson finite difference approach

ABSTRACT

The purpose of this paper is to present an efficient method for pricing discounted American capped options. They differ from the corresponding uncapped ones by the existing trigger level for the underlying asset. In such a way the option's seller is preserved from the possible large movements of the underlying asset. We first obtain the optimal exercise region and by the use of some hitting properties we derive the fair option price. We use the Crank-Nicolson finite difference approach together with a Monte Carlo method to implement the obtained formulas. This method applied for the pricing problem of the ordinary American options has its own significance. Finally, we present some numerical results.

© 2022 Elsevier Ltd. All rights reserved.

1. Introduction

American style options are one of the most traded financial instruments. This gives rise to the strong scientific interest to them. A large number of classical publications are available – we refer to Brennan and Schwartz [1–5]. The increasing financial interest to the American style derivatives motivates many researchers to investigate additionally this area in the recent years. Nunes et al. [6] examine American options under the constant elasticity of variance models. The American option valuation problem in the fractional Black–Scholes market is considered in Chen et al. [7]. The Fourier transform is used in Chan [8,9] for pricing and hedging early-exercise options under the exponential Lévy assumptions. Some jump diffusion models are presented in Deng [10–13]. The American options under the Heston framework are examined in Jeon et al. [14,15]. A model with stochastic spreads is examined in Arregui et al. [16]. Some barrier options are examined in Deng [17–19]. Michael [20] focuses on the so called early exercise premium which is the price of the option's holder early exercise right. Different lookback American style options are studied in Deng [21–

23]. Some finite difference approaches for American option valuation are presented in Soleymani et al. [24–26]. Another numerical method based on a maximization of the option's holder financial results can be found in Zaeveski [27].

To meet the financial investors' expectations for additional protection several instruments are listed at the markets. They preserve the derivative's seller against the extremely high movements of the underlying asset. The so called game style options protect the seller's interest giving him an early exercise right – see Kifer [28–32]. Alternatively, other derivatives preserve the seller by adding a cap level limiting the price of the underlying asset at which the option can be exercised. A seminal work for these options based on the Black–Scholes framework is Broadie and Detemple [33]. Later [34] examines capped options under a general diffusion process. Several researchers use the capped style options to evaluate the ordinary American options – see Broadie and Detemple [35,36].

We add in the present article a new discount factor which influences the amount due from the option's seller. This additional discounting has two major significances. First, in such a way we introduce a time dependence in the option's payment structure. This leads to a benefit for the option's buyer to exercise earlier. On the other hand the option's seller receives an additional protection against large movements of the underlying asset in the more

E-mail address: t_s_zaevski@math.bas.bg

distant future. The second importance is related to the financial models which allow continuously payed dividends of the underlying asset. It is proven in Zaeveski [30], proposition 2.3, that after a parameters' change a model with dividends can be written as a non-dividend model.

Our approach for pricing capped options is based on deriving the option's holder optimal boundary. We prove two theorems for the call and put options. The first one says that the exercise boundary of an American capped call option is the lower between the optimal boundary of the uncapped option and the cap. Analogously, the second theorem states that the optimal boundary of the capped put option is the larger between the cap value and the optimal boundary of the uncapped option. A similar result is obtained in Broadie and Detemple [33]. We have to mention that we prove these two theorems using an approach based on the infinitesimal generators. In such a way the theorems can be easily proven under more general Feller-Markov assumptions. For example, different stochastic volatility models admit such interpretation. We refer to the classical [37] model, considered also in He and Lin [38], as well as to its extensions of Bates [39,40] which incorporate a jump behavior. Another jump stochastic volatility model is defined and examined in He and Lin [41] – the jumps are presented by a Lévy stable process. Other extensions of the Heston's model are published recently in He and Chen [42,43]. The first one introduces regime switching in the volatility, whereas the second article assumes that the long-term mean of the volatility is stochastic.

Using the approach presented in Zaeveski [27] we can approximate the exercise boundary of the uncapped option. Hence, we can obtain the early exercise boundary of the capped option using the mentioned above theorems. It divides the state space of the underlying asset into two parts – the continuation region and the early exercise region. In the first one it is optimal for the holder to keep the option, whereas in the second one the immediate exercise leads to a better financial result. It is well known that pricing of an American style derivative is closely related to a free boundary problem arising from the necessity of identifying the optimal stopping moment. Since we have approximated the exercise boundary, we arrive to a partial differential equation (PDE, hereafter) which holds in a known region – namely the continuation region. The form of the exercise boundary of the capped option leads to a (semi-)closed formulas for the prices. They consist of a part related to the first hitting moment of the underlying asset to the cap and conceivably of the averaged prices of some uncapped American options. In some cases the capped and uncapped options may coincide. We use a finite difference approach to solve the PDE for the uncapped American options. This method is chosen because it obtains all prices at once which reduces the computational time significantly. Particularly, we use the version of Crank and Nicolson [44]. It has some major advantages. First, it has been developed namely for the heat style equations. Second, this method has a very fast convergence avoiding some possible oscillations in addition. The available boundary constraints for the put options, whether capped or uncapped, are only at the lower and the right boundaries since the continuation region is open above. Usually the put option price is set to be zero for some large value of the underlying asset when a finite difference scheme is used. Unfortunately, this assumption has a major disadvantage – this value has to be extremely large for longer maturities. To avoid this inconvenience we obtain the option prices for a suitable value of the underlying asset using a Monte Carlo method presented in Zaeveski [27] (the second one). This method is relatively fast and accurate. The produced prices are used for the upper boundary constraint. The same modification of the finite difference approach is helpful for a time reduction when we consider a call option with a large strike or a large exercise boundary. At last but not least, some numerical results are presented. We compare the capped

and uncapped prices as well as the so called premium for capping. It presents the price which the option's seller pays for the cap feature, i.e. the difference between the prices of the American uncapped and capped options. Here is the place to note another importance of the mentioned above Crank–Nicolson numerical method. Using it we obtain jointly the prices of the capped and uncapped options which significantly reduces the time consumption. Also, this algorithm provides the prices for all maturities below some moment and different cap values.

The paper is structured in the following way. In Section 2 we present the base we shall use later. In Sections 3 and 4 we present the derived results for the put and call options, respectively. In Appendix A are given some useful proposition related to the Brownian motion's first hitting time.

2. Preliminaries

Let the underlying asset price be driven by a geometric Brownian motion

$$S_t = S_0 \exp \left(\left(r - \frac{\sigma^2}{2} \right) t + \sigma B_t \right) \quad (2.1)$$

under the filtered probability space $(\Omega, \mathcal{F}, \mathcal{F}_t, Q)$. The probability measure is assumed to be risk-neutral. We shall denote by \mathcal{A} the infinitesimal generator

$$(\mathcal{A}f)(x) = rx f'(x) + \frac{\sigma^2}{2} f''(x). \quad (2.2)$$

We assume for the sake of simplicity that the risk free rate r and the discount rate λ are some constants such that $\lambda \geq 0$ and $r + \lambda > 0$. Note that we do not impose a positiveness of the risk free rate. Let the maturity date be denoted by T , and the option's strike and the cap level be K and L , respectively. If we have a put option then $L < K$ and $L > K$ for call options. We shall use the symbols “ \wedge ” and “ \vee ” for minimum and maximum, i.e. $a \wedge b = \min(a, b)$ and $a \vee b = \max(a, b)$. The functions which describe the payment structure for the discounted American capped call and put options can be written as

$$\begin{aligned} N(t, x) &= e^{-\lambda t} (S_t \wedge L - K)^+ \\ N(t, x) &= e^{-\lambda t} (K - S_t \vee L)^+, \end{aligned} \quad (2.3)$$

respectively. Let us denote by $\mathcal{T}_{[t, T]}$, $t < T$, the set of all stopping times with values in the interval $[t, T]$. Below we define the so called exercise and continuation regions.

Definition 2.1. A point (t, x) belongs to the exercise region Υ if for an arbitrary stopping time $\zeta \in \mathcal{T}_{[t, T]}$

$$N(t, x) \geq E^{t, x} [e^{-r(\zeta-t)} N(\zeta, S_\zeta)]. \quad (2.4)$$

The continuation region $\bar{\Upsilon}$ consists of these points (t, x) for which inequality (2.4) is not true for some stopping time ζ . The boundary between Υ and $\bar{\Upsilon}$ is called early exercise boundary and we denote it by $c(t)$.

We shall use several times the following well known proposition known as a Dynkin's formula.

Proposition 2.1 (Dynkin's formula). *Let τ be a finite stopping time with values not less t . Then we have the following integral representation for the expectation $E^{t, x}[f(\tau, S_\tau)]$*

$$E^{t, x}[f(\tau, S_\tau)] = f(t, x) + E^{t, x} \left[\int_t^\tau f_t(u, S_u) + (\mathcal{A}f)(u, S_u) du \right]. \quad (2.5)$$

The following proposition gives the time structure of the option (capped or uncapped) prices.

Proposition 2.2. Let the price of a live option with maturity date T is denoted by $F(t; T)$. We have for every moment t before the maturity

$$F(t; T) = e^{-\lambda t} F(0; T - t). \quad (2.6)$$

Proof. Let $\tau \in \mathcal{T}_{[t, T]}$ be the optimal strategy for a live option assuming that at the moment t the underlying asset value is $S_t = x$. Using the Markov property, we obtain

$$\begin{aligned} F(t; T) &= E^{t,x} [e^{-r(\tau-t)} N(\tau, S_\tau)] \\ &= e^{-\lambda t} E^{0,x} [e^{-r(\tau-t)} N(\tau - t, S_{\tau-t})] \\ &= e^{-\lambda t} F(0; T - t), \end{aligned} \quad (2.7)$$

which finishes the proof. \square

3. Put capped options

Let us consider a put capped option. We shall derive its optimal exercise region and then we shall obtain the option pricing formulas. We shall also present a finite difference approach based on the Crank–Nicolson procedure and we shall apply it for some particular parameters' values.

3.1. Optimal region. Pricing.

Let us denote by Υ^A and $c^A(t)$ the exercise region and the corresponding boundary of the uncapped American option. We can approximate this boundary using the approach presented in Zaeveski [27]. If the boundary is examined w.r.t. the time to maturity, it is proven that the function $c^A(t)$ starts (proposition 3.5) from the value

$$D_1 = \min \left(\frac{r + \lambda}{\lambda}, 1 \right) K \quad (3.1)$$

and decreases to the perpetual value (Theorem 6.2)

$$D_2 = \frac{\gamma}{\gamma + 1} K \quad (3.2)$$

for

$$\gamma = \sqrt{\left(\frac{r}{\sigma^2} - \frac{1}{2} \right)^2 + 2 \frac{r + \lambda}{\sigma^2}} + \left(\frac{r}{\sigma^2} - \frac{1}{2} \right). \quad (3.3)$$

The following theorem determines the exercise boundary of the capped option.

Theorem 3.1. The exercise boundary of the discounted American capped put option is

$$c(t) = c^A(t) \vee L. \quad (3.4)$$

Proof. Suppose first that for some t and $x > L$, the point $(t, x) \in \Upsilon^A$. Note that x has to be smaller than the strike, $x < K$. Hence, for every stopping time ζ from the set $\mathcal{T}_{[t, T]}$

$$\begin{aligned} (K - x \vee L) &\equiv (K - x) \geq E^{t,x} \left[e^{-(r+\lambda)(\zeta-t)} (K - S_\zeta)^+ \right] \\ &\geq E^{t,x} \left[e^{-(r+\lambda)(\zeta-t)} (K - S_\zeta \vee L)^+ \right]. \end{aligned} \quad (3.5)$$

Therefore the point $(t, x) \in \Upsilon$ too. The next step is to prove that all points below the cap level are optimal. Suppose that for some t and $x < L$, we have that $(t, x) \in \Upsilon$. Therefore there exists a stopping time $\zeta \in \mathcal{T}_{[t, T]}$ which gives a better result for the option's holder than the immediate exercise. We have $S_\zeta < K$, because in the opposite case the option's holder will receive nothing. Hence,

$$\begin{aligned} K - L &\equiv K - x \vee L < E^{t,x} \left[e^{-(r+\lambda)(\zeta-t)} (K - S_\zeta \vee L)^+ \right] \\ &= E^{t,x} \left[e^{-(r+\lambda)(\zeta-t)} (K - S_\zeta \vee L) \right] \\ &< E^{t,x} \left[e^{-(r+\lambda)(\zeta-t)} (K - L) \right] \\ &< K - L. \end{aligned} \quad (3.6)$$

We have used above that $r + \lambda > 0$. The contradiction shows that the points below the cap level L are optimal. It remains to prove that all points (t, x) , such that $x > L \vee c^A(t)$, are not optimal. We shall use an approach similar to one presented in Broadie and Detemple [33].

Suppose that $(t, x) \in \Upsilon$ and $x > L \vee c^A(t)$. Let us note first that if $L \leq D_2$ we have that $L < c(t)$ for every t . This is true because D_2 is just $c^A(\infty)$ and the optimal boundary for an American put decreases w.r.t. the time to maturity. Hence, the capped option is ordinary American and the theorem is proven. Suppose now that $D_2 < L < D_1$. Therefore there exists an ordinary American option with shorter maturity, say $\bar{T} < T$, such that its optimal boundary is above the cap level L at the moment t , $L < \bar{c}^A(t)$. Thus we conclude that the point (t, x) is not optimal for the new option. Something more if ζ is the first hitting time to $\bar{c}^A(t)$ if it happens before \bar{T} and \bar{T} otherwise, then

$$K - x < E^{t,x} \left[e^{-(r+\lambda)(\zeta-t)} (K - S_\zeta)^+ \right]. \quad (3.7)$$

Since $S_\zeta > L$, inequality (3.7) shows that the strategy ζ gives a better financial result for the holder of the original capped option than the immediate exercise and therefore the point $(t, x) \notin \Upsilon$.

Suppose now that $L \geq D_1$. Note that this is possible only when $r < 0$ which leads to $D_1 < K$. Let ζ be the lower between the first hitting moment of the underlying asset to the value L and the maturity date T . We shall use the equality $(K - x)^+ = (K - x) + (x - K)I_{x \geq K}$ as well as Dynkin's formula (2.5) to obtain the following statement.

$$\begin{aligned} E^{t,x} [e^{-r(\zeta-t)} N(\zeta, S_\zeta)] &= E^{t,x} [e^{-r(\zeta-t)} e^{-\lambda \zeta} (K - S_\zeta)^+] \\ &= E^{t,x} [e^{-r(\zeta-t)} e^{-\lambda \zeta} (K - S_\zeta)] + E^{t,x} [e^{-r(\zeta-t)} e^{-\lambda \zeta} (S_\zeta - K)I_{S_\zeta \geq K}] \\ &\quad \pm e^{-\lambda t} (K - x) \\ &= e^{-\lambda t} (K - x) + E^{t,x} [e^{-r(\zeta-t)} e^{-\lambda \zeta} (S_\zeta - K)I_{S_\zeta \geq K}] \\ &\quad + E^{t,x} [K(e^{-r(\zeta-t)} - e^{-\lambda t})] - E^{t,x} [S_\zeta e^{-r(\zeta-t)} - \lambda \zeta] + x e^{-\lambda t} \\ &= e^{-\lambda t} (K - x) + E^{t,x} [e^{-r(\zeta-t)} e^{-\lambda \zeta} (S_\zeta - K)I_{S_\zeta \geq K}] \\ &\quad + E^{t,x} \left[K \int_t^\zeta -(r + \lambda) e^{-\lambda u - r(u-t)} du \right] - x e^{-\lambda t} \\ &\quad - E^{t,x} \left[\int_t^\zeta -\lambda e^{-r(u-t) - \lambda u} S_u du \right] + x e^{-\lambda t} \\ &= e^{-\lambda t} (K - x) + E^{t,x} [e^{-r(\zeta-t)} e^{-\lambda \zeta} (S_\zeta - K)I_{S_\zeta \geq K}] \\ &\quad + E^{t,x} \left[\int_t^\zeta e^{-r(u-t) - \lambda u} (\lambda S_u + (r + \lambda)K) du \right] \\ &> e^{-\lambda t} (K - x). \end{aligned} \quad (3.8)$$

The last inequality is true because (A) the first expectation is always positive and (B) the integral is positive since $S_u > L > D_1$ for $u < \zeta$ which is equivalent to $\lambda S_u > (r + \lambda)K$. The contradiction between inequality (3.8) and Definition 2.1 is due to the assumption $(t, x) \in \Upsilon$. This finishes the proof. \square

Remark 3.1. Let us mention that the similar approach as above can be used if the model is stated under significantly general assumptions. First, if we consider a general diffusion model, then its drift under the risk-neutral measure has to be again rS_t . We have applied above Dynkin's formula (2.5) to the function

$$f(u, x) = x e^{-r(u-t) - \lambda u}. \quad (3.9)$$

Since it is linear w.r.t. the variable x , only the first derivative influences its infinitesimal generator. Hence, conclusions (3.8) are true

for the general diffusion models too and therefore [Theorem 3.1](#) still holds.

More generally, if the underlying asset is driven by some Feller-Markov process, we can use an analogue of [Proposition 2.1](#). Hence, scheme (3.8) can be used again with the corresponding form of the infinitesimal generator.

Hereafter, we assume $t = 0$ referring to [Proposition 2.2](#). If $L \in [D_1, K)$ (this is possible only when $r < 0$) then the exercise boundary is the cap value L . If the asset starts below L then the option price is simply $F = K - L$. Suppose now that $S_0 > L$. We shall use the results of [\[45\]](#) for the Laplace transforms of the first hitting time – we present them in [Appendix A](#). Note that there hitting is assumed to be above. Hence we have to examine the opposite Brownian motion $\bar{B}_t = -B_t$ instead the original one. Let ζ be the first hitting moment of the underlying asset to L or equivalently, the hitting of the opposite Brownian motion to the linear function $b(t) = b_1 t + b_2$ for

$$\begin{aligned} b_1 &= \frac{r}{\sigma} - \frac{\sigma}{2} \\ b_2 &= \frac{\ln S_0 - \ln L}{\sigma}. \end{aligned} \quad (3.10)$$

Therefore the option price is

$$\begin{aligned} F &= E[e^{-(r+\lambda)\zeta} (K - L) I_{\zeta \leq T}] + E[e^{-(r+\lambda)T} (K - S_T)^+ I_{\zeta > T}] \\ &= (K - L) E[e^{-(r+\lambda)\zeta} I_{\zeta \leq T}] + K e^{-(r+\lambda)T} E[I_{\zeta > T, S_T < K}] \\ &\quad - S_0 e^{-(\lambda + \frac{\sigma^2}{2})T} E[e^{\sigma B_T} I_{\zeta > T, S_T < K}]. \end{aligned} \quad (3.11)$$

Using propositions [Appendix A.1](#) and [Appendix A.2](#) ([Theorems 3.1](#) and [3.2](#) from Zaeviski [\[45\]](#)) we conclude

$$\begin{aligned} F &= (K - L) e^{b_2(\sqrt{b_1^2 + 2(r+\lambda)} - b_1)} g(T, \sqrt{b_1^2 + 2(r+\lambda)}, b_2) \\ &\quad + K e^{-(r+\lambda)T} V(0, d(T, K), T; b_1, b_2) \\ &\quad - S_0 e^{-(\lambda + \frac{\sigma^2}{2})T} V(-\sigma, d(T, K), T; b_1, b_2), \end{aligned} \quad (3.12)$$

where the functions $g(\cdot)$, $d(\cdot)$ and $V(\cdot)$ are

$$\begin{aligned} g(T; b_1, b_2) &= 1 - N\left(\frac{b_1 T + b_2}{\sqrt{T}}\right) + \exp(-2b_1 b_2) N\left(\frac{b_1 T - b_2}{\sqrt{T}}\right) \\ d(t, x) &= \frac{\ln S_0 - \ln x}{\sigma} + \left(\frac{r}{\sigma} - \frac{\sigma}{2}\right)t \\ &\quad V(\theta, z, T; b_1, b_2) \\ &= \exp\left(\frac{T\theta^2}{2}\right) \left[N\left(\frac{b(T) - T\theta}{\sqrt{T}}\right) - N\left(\frac{z - T\theta}{\sqrt{T}}\right) \right. \\ &\quad \left. + e^{2b_2(\theta - b_1)} \left(N\left(\frac{z - T\theta - 2b_2}{\sqrt{T}}\right) - N\left(\frac{b(T) - T\theta - 2b_2}{\sqrt{T}}\right) \right) \right]. \end{aligned} \quad (3.13)$$

Suppose now that $L \in (D_2, D_1)$. Let us denote by τ^* this time to maturity, for which $c(\tau^*) = L$. If $T \leq \tau^*$, then the option turns to an ordinary American put. Suppose now that $T > \tau^*$. Therefore $c(t) = L$ for $t < T - \tau^*$ and $c(t) = c^A(t)$ for $t \geq T - \tau^*$. Let the function $f(\cdot)$ be defined as

$$f(t, y) = \frac{1}{\sqrt{2\pi t}} \left(1 - \exp\left(-\frac{2b_2(b(t) - y)}{t}\right) \right) \exp\left(-\frac{y^2}{2t}\right). \quad (3.14)$$

Let us denote by $A(y, \tau)$ the price of an ordinary American put if the asset starts from the value y and the time to maturity is τ . Using [Propositions 2.2](#) and [Appendix A.3](#) ([Eq. \(3.7\)](#) from Zaeviski [\[45\]](#)) we conclude that the option price can be presented as

$$\begin{aligned} F &= E[e^{-(r+\lambda)\zeta} (K - L) I_{\zeta \leq T - \tau^*}] + e^{-r(T - \tau^*)} \int_{-d(T - \tau^*, L)}^{\infty} A\left(S_0 e^{(r - \frac{\sigma^2}{2})(T - \tau^*) + \sigma y}, \tau^*\right) dQ(B_{T - \tau^*} < y, \zeta > T - \tau^*) \\ &= E[e^{-(r+\lambda)\zeta} (K - L) I_{\zeta \leq T - \tau^*}] + e^{-(r+\lambda)(T - \tau^*)} \int_{-d(T - \tau^*, L)}^{\infty} A\left(S_0 e^{(r - \frac{\sigma^2}{2})(T - \tau^*) - \sigma y}, \tau^*\right) f(T - \tau^*, y) dy. \end{aligned} \quad (3.15)$$

Finally, note that if $L \leq D_2$, then the optimal exercise boundary of the pure American option is always above the cap level. Therefore the capped option turns to an ordinary one. We can summarize the derived results in the following theorem.

Theorem 3.2. *The price of an American capped put option can be derived through one of the following statements.*

1. If $L \in [D_1, K)$, then the option price is given by [Eq. \(3.12\)](#) when $S_0 > L$. Otherwise the price is $K - L$.
2. If $L \in (D_2, D_1)$ and $T > \tau^*$, then the price of the American capped option is given by [Eq. \(3.15\)](#) when $S_0 > L$. Otherwise the price is $K - L$.
3. If $L \leq D_2$ or $L \in (D_2, D_1) \cap T \leq \tau^*$, then the option is an ordinary American put and its price can be found using [\[27\]](#).

As a corollary of [Theorem 3.2](#) we provide the result in the perpetual case, i.e. when $T = \infty$

Corollary 3.1. *Suppose that $T = \infty$. Then the early exercise boundary is the line $C = L \vee D_2$. If the asset starts above it, $S_0 > C$, the option price is*

$$F = (K - C) \left(\frac{C}{S_0} \right)^\gamma, \quad (3.16)$$

where γ is given by [Eq. \(3.3\)](#). Otherwise, if $S_0 \leq C$, then the option price is $F = K - S_0$.

Proof. The proof is an immediate consequence from [Theorem 3.2](#) and theorem 6.2 from Zaeviski [\[27\]](#). \square

Let us comment the result of [Corollary 3.1](#) having in mind [Theorem 3.2](#). If $L \geq D_1$, we use [Eq. \(3.12\)](#). Since $T = \infty$, the last two terms vanish and the first one leads to formula (3.16) – note that $C = L$. If $L \in (D_2, D_1)$, then we use [Eq. \(3.15\)](#). Note that always $T > \tau^*$. The second term vanishes due to the discount factor. The first term leads to formula (3.16). Finally, if $L \leq D_2$, then the option is a perpetual American and therefore we have to use theorem 6.2 from Zaeviski [\[27\]](#).

3.2. The Crank–Nicolson finite difference method for American option pricing

We shall construct now a finite difference approach for pricing an American uncapped option solving numerically the correspondent Black–Scholes equation in the approximated region. This equation is closely related to the classical heat equation. The main finite difference algorithms for its solving are the explicit, implicit, and Crank–Nicolson methods. The first one is relatively fast, but it may diverge when the ratio between the time step and the square of the space step is larger than 0.5. The accuracy is proportional to the time step and the square of the state one. The same is true for the implicit algorithm. Differently to the explicit one, it converges ever, but it has a larger time consumption due to the appearing linear system which has to be solved. The main advantage of the Crank–Nicolson method is that the accuracy is proportional to the

square of the space step as well as the square of the time step. Also, this algorithm is always numerical stable and convergent.

Let us find the critical value for the Black–Scholes equation below which the explicit method is stable. Let the constants A , B , α , and β be defined as

$$\begin{aligned} A &= \frac{\sigma^2}{2} \\ B &= r - \frac{\sigma^2}{2} \\ \alpha &= \frac{B}{2A} = \frac{r}{\sigma^2} - \frac{1}{2} \\ \beta &= \frac{B^2}{4A} + r = \frac{1}{2} \left(\frac{r}{\sigma^2} + \frac{1}{2} \right)^2 \end{aligned} \quad (3.17)$$

After the change of variables $u = A(T - t)$ and $y = \ln(x)$ the solution of the Black–Scholes equation $F(t, x)$ can be written as

$$F(t, x) = x^{-\alpha} e^{-\beta(T-t)} f(A(T-t), \ln(x)), \quad (3.18)$$

where the function $f(u, y)$ solves the heat equation $f_u = f_{yy}$. Let us denote by I the length of the state interval in which we solve the Black–Scholes equation and by m and n the time and state steps, respectively. Let also m_{heat} and n_{heat} be the steps for the heat equation $f_u = f_{yy}$. The change of variables above leads to the following equivalence of the stability condition

$$\frac{m_{heat}}{n_{heat}^2} < \frac{1}{2} \Leftrightarrow \frac{m}{n^2} < \frac{1}{2A I^2}. \quad (3.19)$$

We have to mention also that the features of the convergence speed is kept.

All this prompts us to choose namely the Crank–Nicolson finite difference approach when we need to solve the appearing heat style Black–Scholes equation related to the uncapped option. First, we use the three steps algorithm presented in Zaeviski [27] to approximate its early exercise boundary. We derive the values in j_1 main nodes. The algorithm produces meanwhile the values in some additional nodes – we denote by j_2 the number of the total different nodes at which we know the exercise boundary. After that we apply a cubic spline interpolation to determine the boundary at the uniform grid with significant more nodes – their number is denoted by j_3 . It turns out that $j_1 = 5$ and $j_3 = 128$ are sufficient to approximate the optimal boundary. In this case the value of j_2 is 15.

The next step is to apply the second Monte Carlo method presented in Zaeviski [27] to determine the option prices for some fixed initial asset value, denoted by H , and different maturities. The value of H will be specified later. We calculate the prices at the same j_1 nodes and interpolate the rest j_3 nodes. We shall denote the values at this upper boundary H by $h(t)$. Having in mind Proposition 2.2 we conclude that the PDE for the American uncapped option turns to

$$\begin{aligned} F_t(t, x) + rx F_x(t, x) + \frac{1}{2} \sigma^2 x^2 F_{xx}(t, x) - rF(t, x) &= 0 \\ F(t, c^A(t)) &= \exp(-\lambda t)(K - c^A(t)), \quad t \in [0, T] \\ F(t, H) &= \exp(-\lambda t)h(t), \quad t \in [0, T] \\ F(T, x) &= \exp(-\lambda T)(K - x)^+, \quad c(T) < x < H. \end{aligned} \quad (3.20)$$

The equation holds in the region $(t, x) \in \{(0, T) \times (c(t), H)\}$ and the boundary constraints are imposed on the lower, upper, and the right boundaries. Since the function $c(t)$ is increasing we shall use the finite difference approach at the region $\{(0, T) \times (c(0), H)\}$. We shall work backwards. We divide the time interval into M points whereas the x -interval is divided into N points – $T \equiv t_1 > t_2 > \dots > t_M \equiv 0$ and $c(0) \equiv x_1 < x_2 < \dots < x_N \equiv H$. We shall denote by $F(m, n)$ our approximation of the solution of Eq. (3.20) in the node (m, n) .

1. We approximate all values of $c(t_m)$, $m = 1, 2, \dots, M$, using a cubic spline interpolation over the calculated above j_3 values of the exercise boundary.
2. For every $m = 1, 2, \dots, M$ we derive the largest value of n for which the point (t_m, x_n) is not above $c(t_m)$. Let this value be l_m . We set $F(m, n) = e^{-\lambda t_m}(K - x_n)$ for every m and $n \leq l_m$.
3. For every $n = 1, 2, \dots, N$ we set $F(1, n) = e^{-\lambda T}(K - x_n)^+$. Note that we work backwards and hence $F(1, n)$ are the values at the maturity.
4. For every $m = 1, 2, \dots, M$ we set $F(m, N) = e^{-\lambda t_m}h(t_m)$.
5. Suppose that we have derived all values $F(j, n)$ for all $j < m$ and an arbitrary n . We approximate the terms in Eq. (3.20) in accordance of the Crank–Nicolson approach

$$\begin{aligned} F_t &= \frac{F(m-1, n) - F(m, n)}{\Delta t} \\ F &= \frac{F(m-1, n) + F(m, n)}{2} \\ F_x &= \frac{F(m-1, n) - F(m-1, n-1) + F(m, n) - F(m, n-1)}{2\Delta x} \\ F_{xx} &= \frac{F(m-1, n+1) - 2F(m-1, n) + F(m-1, n-1)}{2(\Delta x)^2} \\ &\quad + \frac{F(m, n+1) - 2F(m, n) + F(m, n-1)}{2(\Delta x)^2}. \end{aligned} \quad (3.21)$$

In such a way Eq. (3.20) turns to

$$\begin{aligned} 0 &= \frac{F(m-1, n) - F(m, n)}{\Delta t} \\ &\quad + \frac{1}{2} r x_n \frac{F(m-1, n) - F(m-1, n-1) + F(m, n) - F(m, n-1)}{\Delta x} \\ &\quad + \frac{1}{4} \sigma^2 x_n^2 \left(\frac{F(m-1, n+1) - 2F(m-1, n) + F(m-1, n-1)}{(\Delta x)^2} + \frac{F(m, n+1) - 2F(m, n) + F(m, n-1)}{(\Delta x)^2} \right) \\ &\quad - \frac{1}{2} r (F(m-1, n) + F(m, n)). \end{aligned} \quad (3.22)$$

After rearranging Eq. (3.22) we derive the following linear system for $F(m, n)$, $l_m + 1 \leq n \leq N - 1$:

- If $n = l_m + 1$, then

$$\begin{aligned} F(m, n) &\left(\frac{1}{\Delta t} - \frac{1}{2} \frac{r x_n}{\Delta x} + \frac{1}{2} \frac{\sigma^2 x_n^2}{(\Delta x)^2} + \frac{1}{2} r \right) - F(m, n+1) \frac{1}{4} \frac{\sigma^2 x_n^2}{(\Delta x)^2} \\ &= F(m-1, n-1) \left(-\frac{1}{2} \frac{r x_n}{\Delta x} + \frac{1}{4} \frac{\sigma^2 x_n^2}{(\Delta x)^2} \right) \\ &\quad + F(m-1, n) \left(\frac{1}{\Delta t} + \frac{1}{2} \frac{r x_n}{\Delta x} - \frac{1}{2} \frac{\sigma^2 x_n^2}{(\Delta x)^2} - \frac{1}{2} r \right) \\ &\quad + F(m-1, n+1) \frac{1}{4} \frac{\sigma^2 x_n^2}{(\Delta x)^2} \\ &\quad - F(m, l_m) \left(\frac{1}{2} \frac{r x_n}{\Delta x} - \frac{1}{4} \frac{\sigma^2 x_n^2}{(\Delta x)^2} \right). \end{aligned} \quad (3.23)$$

- If $l_m + 1 < n < N - 1$, then

$$\begin{aligned} F(m, n-1) &\left(\frac{1}{2} \frac{r x_n}{\Delta x} - \frac{1}{4} \frac{\sigma^2 x_n^2}{(\Delta x)^2} \right) \\ &\quad + F(m, n) \left(\frac{1}{\Delta t} - \frac{1}{2} \frac{r x_n}{\Delta x} + \frac{1}{2} \frac{\sigma^2 x_n^2}{(\Delta x)^2} + \frac{1}{2} r \right) \\ &\quad - F(m, n+1) \frac{1}{4} \frac{\sigma^2 x_n^2}{(\Delta x)^2} \\ &= F(m-1, n-1) \left(-\frac{1}{2} \frac{r x_n}{\Delta x} + \frac{1}{4} \frac{\sigma^2 x_n^2}{(\Delta x)^2} \right) \\ &\quad + F(m-1, n) \left(\frac{1}{\Delta t} + \frac{1}{2} \frac{r x_n}{\Delta x} - \frac{1}{2} \frac{\sigma^2 x_n^2}{(\Delta x)^2} - \frac{1}{2} r \right) \\ &\quad + F(m-1, n+1) \frac{1}{4} \frac{\sigma^2 x_n^2}{(\Delta x)^2}. \end{aligned} \quad (3.24)$$

- If $n = N - 1$, then

$$\begin{aligned}
 & F(m, n-1) \left(\frac{1}{2} \frac{rx_n}{\Delta x} - \frac{1}{4} \frac{\sigma^2 x_n^2}{(\Delta x)^2} \right) \\
 & + F(m, n) \left(\frac{1}{\Delta t} - \frac{1}{2} \frac{rx_n}{\Delta x} + \frac{1}{2} \frac{\sigma^2 x_n^2}{(\Delta x)^2} + \frac{1}{2} r \right) \\
 & = F(m-1, n-1) \left(-\frac{1}{2} \frac{rx_n}{\Delta x} + \frac{1}{4} \frac{\sigma^2 x_n^2}{(\Delta x)^2} \right) \\
 & + F(m-1, n) \left(\frac{1}{\Delta t} + \frac{1}{2} \frac{rx_n}{\Delta x} - \frac{1}{2} \frac{\sigma^2 x_n^2}{(\Delta x)^2} - \frac{1}{2} r \right) \\
 & + F(m-1, n+1) \frac{1}{4} \frac{\sigma^2 x_n^2}{(\Delta x)^2} + F(m, N) \frac{1}{4} \frac{\sigma^2 x_n^2}{(\Delta x)^2}. \quad (3.25)
 \end{aligned}$$

This system consists of $N - l_m - 1$ linear equations w.r.t. the variables $F(m, l_m + 1), (m, l_m + 2), \dots, F(m, N - 1)$. We derive all values at the m th time node solving it.

6. We repeat this procedure until we find all values $F(m, n)$.

3.3. Numerical method for pricing American capped put options

When we price a capped option we have to modify the approach from Section 3.2. We present below an algorithm which allows us to calculate the price of the capped option as well as the value of its uncapped analogue. In such a way we evaluate the premium for capping. As we have seen in Theorem 3.2 three cases are possible. If $L \leq D_2$ or $L \in (D_2, D_1) \cap T \leq \tau^*$, then capping has no influence, and therefore the capped option turns to a usual American one. On the other hand if $L \in [D_1, K)$, there exists a closed form formula for the capped option price – formula (3.12). The most complicate case is $L \in (D_2, D_1) \cap T > \tau^*$ – it combines the features of both previous cases. Having in mind the remarks above we construct the following algorithm.

1. We use the presented in Section 3.2 approach to derive the exercise boundary of the uncapped option and its price structure w.r.t the time and state divisions.
2. If the exercise boundary at the initial moment is above the cap, $c(t_M) \equiv c(0) \geq L$, then both capped and uncapped options coincide and therefore the task is solved. Remind that we work backwards in the finite difference scheme.
3. If $L \in [D_1, K)$, we have to apply closed form formula (3.12) to obtain the price of the capped option.
4. We consider the case $L \in (c(0), D_1)$. We have to rely now on formula (3.15). Its first part can be derived explicitly. Hence, we have to evaluate its integral part. The rest of the algorithm is intended for this.
5. We derive the lowest m for which $c(t_m) > L$. Let us denote it by \bar{m} . It approximates the value of τ^* , $\tau^* \approx t_{\bar{m}}$.
6. If $\bar{m} = M$, then the optimal boundary is above the cap only at the maturity and hence the option price is approximately equal to formula (3.12).
7. Suppose now $\bar{m} < M$. Remind that $l_{\bar{m}}$ is the largest value of n , for which x_n is not above $c(t_{\bar{m}})$. We use the derived values of $F(n, \bar{m})$, $n = l_{\bar{m}} + 1, \dots, N$ to approximate the price function for the uncapped option which appears in the integral part of formula (3.15) –

$$A \left(S_0 e^{\left(r - \frac{\sigma^2}{2} \right) t_{\bar{m}} - \sigma y}, t_{\bar{m}} \right). \quad (3.26)$$

Note that in the finite difference scheme the x -nodes are for the underlying asset, not for the Brownian motion.

8. Using a cubic spline interpolation we approximate function (3.26) at N_1 uniformly distributed on the interval $(c(t_{\bar{m}}), H)$ nodes.

9. We value function (3.14) at the obtained above x -nodes.
10. We approximate the integral from Eq. (3.15) averaging the product of functions (3.26) and (3.14).
11. We finish our algorithm discounting the integral by $e^{-(r+\lambda)t_{\bar{m}}}$ and summing both parts of formula (3.15).
12. The premium for capping can be obtain as the difference between the prices of the uncapped and capped options.

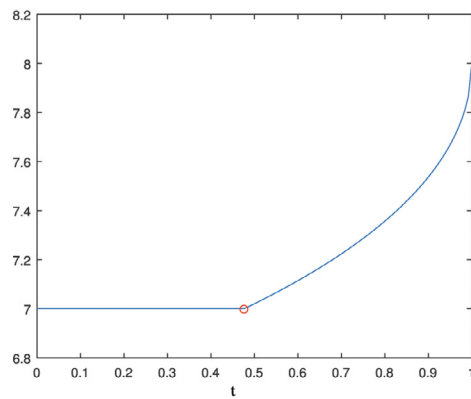
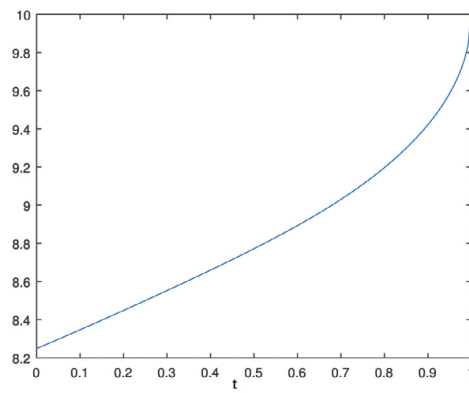
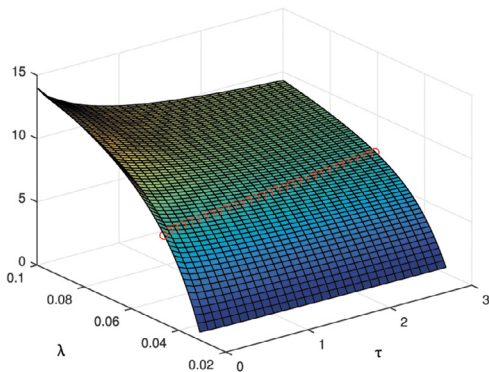
3.4. Numerical results

Both typical forms of the optimal boundary of an American capped put option are presented at Fig. 1a and 1b. We consider a negative risk-free rate of return, $r = -0.03$, because in this case the exercise boundary is below the strike at the maturity. We assume that the option expires after one year, i.e. $T = 1$, the strike price is $K = 20$, the cap level is $L = 7$, and the volatility is $\sigma = 0.3$. For Fig. 1a we use value $\lambda = 0.05$. The terminal values D_1 and D_2 are $D_1 = 8.0000$ and $D_2 = 3.7906$. The critical value for the time to maturity is $\tau^* = 0.5235$ and it is marked by red color in Fig. 1a. Let us assume that $\lambda = 0.06$. The critical values are $D_1 = 10.0000$, $D_2 = 5.0000$, and $\tau^* = 2.8290$. Since $\tau^* > T$ the option turns to an uncapped American put. The boundary can be seen in Fig. 1b.

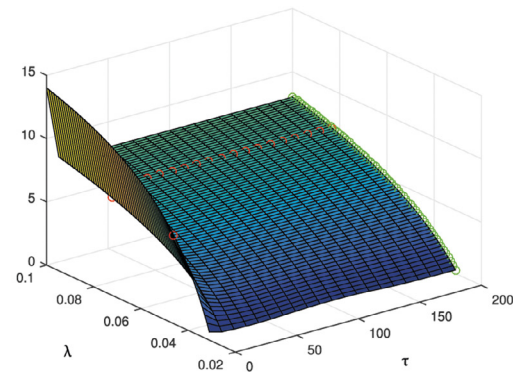
In Fig. 1e and 1c we present the exercise boundaries of the capped and uncapped options varying the time to maturity between zero and three, $\tau \in (0, 3)$, and the discount rate among $\lambda \in (0.031, 0.1)$. Note that these values guarantee $r + \lambda > 0$. We again mark by red color the values at which the boundary turns to the cap. The boundary's behavior for longer maturities can be seen at Fig. 1f and 1d. The time to maturity belongs to the interval $(0, 200)$. The green points are the corresponding perpetual values calculated by the use of Corollary 3.1. We can see that for the longer maturities the boundary's values are very close to the corresponding perpetual ones.

At Fig. 2 we present the behavior of the option prices (with and without capping) and the premium for capping. We separately consider the cases with short and middle maturities on one hand side and with large and extremely large maturities at other. For the first one the time to maturity is assumed to be between $\tau \in (0, 3)$, whereas for the second one we use values larger than $20 - \tau \in (20, 200)$. For both cases we have to derive this value of H which guarantees that the interval $(c(t_{\bar{m}}), H)$ comprises the significant mass of the distribution $f(\cdot)$ from Eq. (3.14). It appears in the integral part of the price formula (3.15). It turns out that for the shorter maturities the sufficient value is $H = 2K = 40$, whereas for the longer ones we need a larger value $H = 10K = 200$. The time interval is divided into $M = 2000$ steps. To use a relatively equal size of the state grid we use $N = 200$ and $N = 1000$ point divisions, respectively, for the short and long maturities. Also, to evaluate correctly the integral in formula (3.15) we divide the interval $(c(t_{\bar{m}}), H)$ into $N_1 = 500^1$ pieces for which we use the cubic spline interpolation. At Fig. 2a, 2c, and 2e are presented the uncapped, capped option prices, and the premium for capping, respectively. We observe that for small values of the discount factor λ the cap is above the optimal boundary value at the maturity, $L > D_1$. Hence we price the capped options via formula (3.12). For larger values of λ the cap is below the terminal boundary value, but it is above its initial value, $c(0) < L < D_1$. Hence we have to use formula (3.15). For even greater values of λ the optimal boundary for the uncapped option is always above the cap and hence both of capped and uncapped options coincide. Particularly, the premium for capping turns to zero. We marked by red and yellow points the critical values of the discount factor at which the capped option changes its feature. Note that the first critical value for the discount factor λ can be calculated explicitly since it leads to $D_1 = L$.

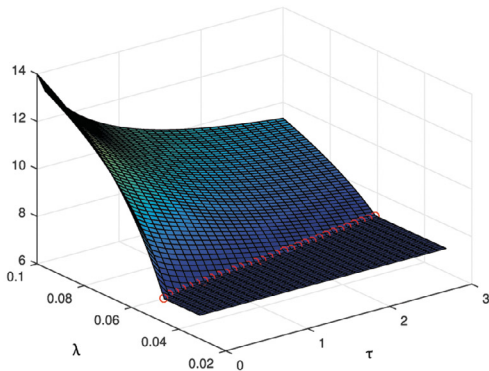
¹ For the shorter maturities we can use $N_1 = 200$.

(a) The optimal boundary, $\lambda = 0.05$.(b) The optimal boundary, $\lambda = 0.06$.

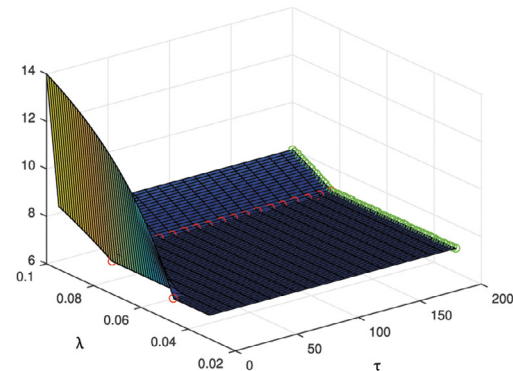
(c) The surface of the uncapped boundary – short maturities.



(d) The surface of the uncapped boundary – long maturities.



(e) The surface of the capped boundary – short maturities.



(f) The surface of the capped boundary – long maturities.

Fig. 1. Put capped options.

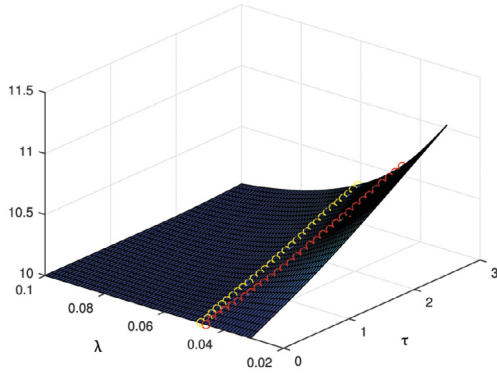
Hence

$$\lambda_1 = -\frac{rK}{K-L}. \quad (3.27)$$

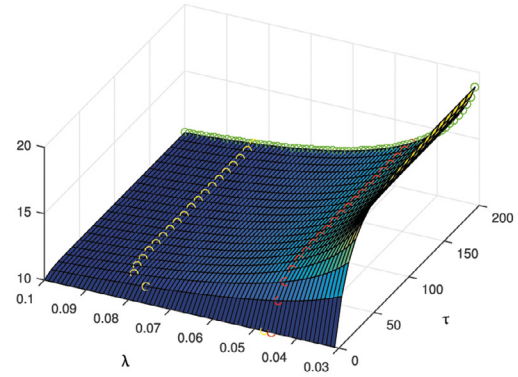
Remind that the risk-free rate is negative. Let us mention that if the time to maturity is zero, $c(0) \equiv D_1$ and therefore both critical values coincide. This can be viewed at Fig. 2. Assumed parameters lead to $\lambda_1 = 0.0462$. At Fig. 2b and 2d we present the price behavior of the long maturing uncapped and capped options. The premium for capping can be seen in Fig. 2f. The perpetual values

calculated explicitly via Corollary 3.1 are plotted again by a green color. We can see that both prices and the premium tend to the perpetual values for large times to maturity.

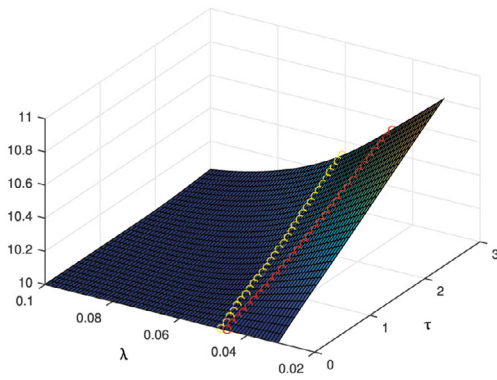
The option prices for some particular values of the parameters are presented in Table 1. We assume again $r = -0.03$, $\sigma = 0.3$, and $K = 20$. The considered options are at-the-money, i.e. $S_0 \equiv K = 20$. We vary the time to maturity as $\tau \in \{0.5, 1, 2, 3\}$, the cap as $L \in \{10, 12, 14, 16, 18\}$, and the discount factor among $\lambda \in \{0.0031, 0.04, 0.05, 0.06, 0.07, 0.08, 0.09, 0.1\}$. The first column presents the prices of the uncapped American options. It



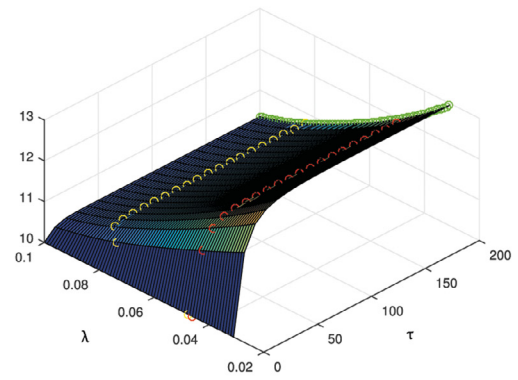
(a) Pure American put option prices, short maturities



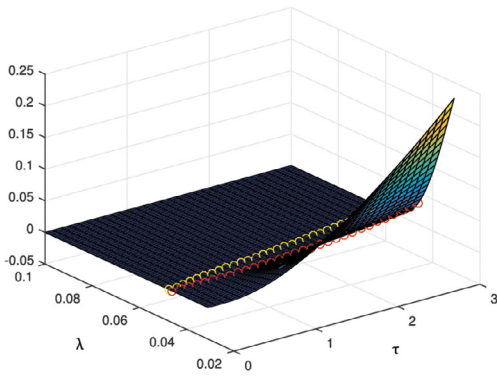
(b) Pure American put option prices, long maturities



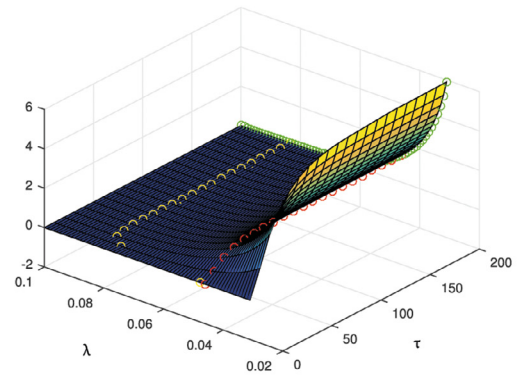
(c) American capped put option prices, short maturities



(d) American capped put option prices, long maturities



(e) Put premium, short maturities



(f) Put premium, long maturities

Fig. 2. Put option prices.

turns out that due to the Monte Carlo modification a relatively low number of the grid nodes are enough for very precise results – $M = 5000$ time and $N = 1000$ state nodes. We use a $N_1 = 500$ -step division for the integral interpolation in formula (3.15). Right to the option prices we mark which formula is valid – “1” if we use formula (3.12), “2” for formula (3.15), and “3” if the capped option coincides with the corresponding uncapped one.

4. Call style options

Since the call and put early exercise boundaries are symmetric in some sense, we shall present the results for call capped options mentioning the differences. We shall use the same notations as above. The value of the exercise boundary of the corresponding uncapped option at the maturity D_1 and the perpetual value D_2

Table 1
Put option prices.

$\lambda = 0.031$	American	$L = 10$	$L = 12$	$L = 14$	$L = 16$	$L = 18$
$\tau = 0.5$	1.8291	1.8289/1	1.8281/1	1.8208/1	1.7654/1	1.3750/1
$\tau = 1$	2.6541	2.6518/1	2.6395/1	2.5847/1	2.3456/1	1.5829/1
$\tau = 2$	3.8695	3.8361/1	3.7521/1	3.5040/1	2.8948/1	1.7394/1
$\tau = 3$	4.8280	4.7169/1	4.5121/1	4.0457/1	3.1693/1	1.8091/1
$\lambda = 0.04$	American	$L = 10$	$L = 12$	$L = 14$	$L = 16$	$L = 18$
$\tau = 0.5$	1.8209	1.8207/1	1.8201/1	1.8136/1	1.7603/1	1.3729/1
$\tau = 1$	2.6303	2.6287/1	2.6187/1	2.5685/1	2.3357/1	1.5795/1
$\tau = 2$	3.8004	3.7774/1	3.7051/1	3.4713/1	2.8769/1	1.7339/1
$\tau = 3$	4.6995	4.6224/1	4.4407/1	3.9986/1	3.1449/1	1.8021/1
$\lambda = 0.05$	American	$L = 10$	$L = 12$	$L = 14$	$L = 16$	$L = 18$
$\tau = 0.5$	1.8117	1.8117/1	1.8112/1	1.8057/1	1.7548/1	1.3707/1
$\tau = 1$	2.6041	2.6033/1	2.5958/1	2.5507/1	2.3247/1	1.5756/1
$\tau = 2$	3.7258	3.7134/1	3.6537/1	3.4354/1	2.8571/1	1.7279/1
$\tau = 3$	4.5645	4.5198/1	4.3630/1	3.9472/1	3.1182/1	1.7943/1
$\lambda = 0.06$	American	$L = 10$	$L = 12$	$L = 14$	$L = 16$	$L = 18$
$\tau = 0.5$	1.8027	1.8026/1	1.8023/1	1.7978/1	1.7492/1	1.3684/1
$\tau = 1$	2.5783	2.5782/1	2.5732/1	2.5330/1	2.3138/1	1.5718/1
$\tau = 2$	3.6554	3.6506/1	3.6032/1	3.4001/1	2.8376/1	1.7219/1
$\tau = 3$	4.4427	4.4198/1	4.2870/1	3.8968/1	3.0919/1	1.7867/1
$\lambda = 0.07$	American	$L = 10$	$L = 12$	$L = 14$	$L = 16$	$L = 18$
$\tau = 0.5$	1.7937	1.7938/2	1.7936/1	1.7900/1	1.7437/1	1.3661/1
$\tau = 1$	2.5533	2.5531/2	2.5507/1	2.5154/1	2.3030/1	1.5680/1
$\tau = 2$	3.5905	3.5889/2	3.5534/1	3.3652/1	2.8183/1	1.7159/1
$\tau = 3$	4.3332	4.3225/2	4.2127/1	3.8473/1	3.0660/1	1.7791/1
$\lambda = 0.08$	American	$L = 10$	$L = 12$	$L = 14$	$L = 16$	$L = 18$
$\tau = 0.5$	1.7849	1.7849/3	1.7845/2	1.7821/1	1.7381/1	1.3639/1
$\tau = 1$	2.5295	2.5295/2	2.5279/2	2.4980/1	2.2922/1	1.5643/1
$\tau = 2$	3.5306	3.5300/2	3.5043/2	3.3308/1	2.7992/1	1.7100/1
$\tau = 3$	4.2333	4.2286/2	4.1399/2	3.7986/1	3.0404/1	1.7717/1
$\lambda = 0.09$	American	$L = 10$	$L = 12$	$L = 14$	$L = 16$	$L = 18$
$\tau = 0.5$	1.7762	1.7762/3	1.7760/2	1.7744/1	1.7326/1	1.3616/1
$\tau = 1$	2.5068	2.5068/3	2.5061/2	2.4807/1	2.2815/1	1.5605/1
$\tau = 2$	3.4746	3.4743/2	3.4562/2	3.2968/1	2.7803/1	1.7041/1
$\tau = 3$	4.1408	4.1385/2	4.0687/2	3.7508/1	3.0152/1	1.7643/1
$\lambda = 0.1$	American	$L = 10$	$L = 12$	$L = 14$	$L = 16$	$L = 18$
$\tau = 0.5$	1.7677	1.7677/3	1.7677/2	1.7663/2	1.7271/1	1.3594/1
$\tau = 1$	2.4852	2.4852/3	2.4848/2	2.4631/2	2.2709/1	1.5568/1
$\tau = 2$	3.4219	3.4218/2	3.4091/2	3.2632/2	2.7617/1	1.6983/1
$\tau = 3$	4.0544	4.0528/2	3.9992/2	3.7039/2	2.9904/1	1.7570/1

now are given by

$$\begin{aligned}
 D_1 &= \max\left(\frac{r+\lambda}{\lambda}, 1\right)K \\
 D_2 &= \frac{\gamma}{\gamma-1}K \\
 \gamma &= \sqrt{\left(\frac{r}{\sigma^2} - \frac{1}{2}\right)^2 + 2\frac{r+\lambda}{\sigma^2}} - \left(\frac{r}{\sigma^2} - \frac{1}{2}\right).
 \end{aligned} \tag{4.1}$$

Since the optimal exercise boundary of the uncapped call option is an increasing function w.r.t. the time to maturity, it has to intersect the capped level in case $D_1 < L < D_2$. We shall denote this moment with τ^* again. Now we shall establish the theorem which gives the form of the early exercise boundary for the capped call options.

Theorem 4.1. *The exercise boundary of an American call capped option is $c(t) = c^A(t) \wedge L$.*

Proof. Suppose first that for some t and $x \in (K, L)$, we have $(t, x) \in \Upsilon^A$. Therefore, for an arbitrary strategy $\zeta \in \mathcal{T}_{[t, T]}$

$$\begin{aligned}
 (x \wedge L - K) &\equiv (x - K) \geq E^{t,x} \left[e^{-(r+\lambda)(\zeta-t)} (S_\zeta - K)^+ \right] \\
 &\geq E^{t,x} \left[e^{-(r+\lambda)(\zeta-t)} (S_\zeta \wedge L - K)^+ \right].
 \end{aligned} \tag{4.2}$$

Hence $(t, x) \in \Upsilon$ too. Suppose that $(t, x) \in \overline{\Upsilon}$ for some t and $x > L$. Therefore there exists a strategy ζ which leads to a larger profit than the immediate exercise. Note that $S_\zeta > K$, because otherwise the option's holder receives nothing. Thus

$$\begin{aligned}
 L - K &\equiv x \wedge L - K < E^{t,x} \left[e^{-(r+\lambda)(\zeta-t)} (S_\zeta \wedge L - K)^+ \right] \\
 &= E^{t,x} \left[e^{-(r+\lambda)(\zeta-t)} (S_\zeta \wedge L - K) \right] \\
 &< E^{t,x} \left[e^{-(r+\lambda)(\zeta-t)} (L - K) \right] \\
 &< L - K.
 \end{aligned} \tag{4.3}$$

Hence $(t, x) \in \Upsilon$. It remains to prove that all points below the contour $c^A(t) \wedge L$ are not optimal for early exercising. Suppose the contrary, i.e. there exists a point $(t, x) \in \Upsilon$ such that $x < c^A(t) \wedge L$. If $L \geq D_2 \equiv c^A(\infty)$, then $c^A(t) \wedge L \equiv c^A(t)$. On the other hand in this case the capped option coincides with an ordinary American option and therefore the theorem is true. Suppose now that $D_1 < L < D_2$. Hence, there exists an option with a shorter maturity \bar{T} , which optimal exercise boundary is below the capped level, $\bar{c}^A(t) < L$. Let us examine a strategy ζ which is the first hitting time to the contour $\bar{c}^A(t) \wedge \bar{T}$. We have that

$$K - x < E^{t,x} \left[e^{-(r+\lambda)(\zeta-t)} (S_\zeta - K)^+ \right]. \quad (4.4)$$

Obviously $\zeta \in \mathcal{T}_{[t,T]}$. Also, having in mind that $S_\zeta < L$ and inequality (4.4) we conclude that the strategy ζ is better for the holder of the original option than immediate exercising. Therefore the point (t, x) can not be optimal.

Finally, we have to examine the case $L \leq D_1$, which is possible only when $r > 0$. We shall examine a strategy ζ which is the first hitting time to the cap if it happens before T , and T otherwise. Using the equality $(x - K)^+ = (x - K) + (K - x)I_{x \leq K}$ and Dynkin's formula (2.5) we derive

$$\begin{aligned} E^{t,x} \left[e^{-r(\zeta-t)} N(\zeta, S_\zeta) \right] &= E^{t,x} \left[e^{-r(\zeta-t)} e^{-\lambda\zeta} (S_\zeta - K)^+ \right] \\ &= E^{t,x} \left[e^{-r(\zeta-t)} e^{-\lambda\zeta} (S_\zeta - K) \right] + E^{t,x} \left[e^{-r(\zeta-t)} e^{-\lambda\zeta} (K - S_\zeta) I_{S_\zeta \leq K} \right] \\ &\quad \pm e^{-\lambda t} (x - K) \\ &= e^{-\lambda t} (x - K) + E^{t,x} \left[e^{-r(\zeta-t)} e^{-\lambda\zeta} (K - S_\zeta) I_{S_\zeta \leq K} \right] \\ &\quad - E^{t,x} \left[K (e^{-r(\zeta-t)-\lambda\zeta} - e^{-\lambda t}) \right] + E^{t,x} \left[S_\zeta e^{-r(\zeta-t)-\lambda\zeta} \right] - x e^{-\lambda t} \\ &= e^{-\lambda t} (x - K) + E^{t,x} \left[e^{-r(\zeta-t)} e^{-\lambda\zeta} (K - S_\zeta) I_{S_\zeta \leq K} \right] \\ &\quad + E^{t,x} \left[K \int_t^\zeta (r + \lambda) e^{-\lambda u - r(u-t)} du \right] + x e^{-\lambda t} \\ &\quad + E^{t,x} \left[\int_t^\zeta -\lambda e^{-r(u-t) - \lambda u} S_u du \right] - x e^{-\lambda t} \\ &= e^{-\lambda t} (x - K) + E^{t,x} \left[e^{-r(\zeta-t)} e^{-\lambda\zeta} (K - S_\zeta) I_{S_\zeta \leq K} \right] \\ &\quad + E^{t,x} \left[\int_t^\zeta e^{-r(u-t) - \lambda u} (-\lambda S_u + (r + \lambda)K) du \right] \\ &> e^{-\lambda t} (x - K). \end{aligned} \quad (4.5)$$

The last inequality is true since for every $u < \zeta$ we have

$$S_u < L < D_1 = \frac{r + \lambda}{\lambda} K. \quad (4.6)$$

We conclude that the point (t, x) can not be optimal since the strategy ζ leads to a better result. \square

We shall prove now the analogue of theorem (3.2). Let the constants b_1 and b_2 , and the functions $g(\cdot)$, $V(\cdot)$, and $d(\cdot)$ be defined again by the equalities (3.10) and (3.13). The price of the uncapped call option shall be denoted by $A(\cdot)$.

Theorem 4.2. If $L \in (K, D_1]$ then $c(t) \equiv L$. If $x \geq L$, then $F = L - K$. Otherwise, if $x < L$, then

$$\begin{aligned} F &= (L - K) e^{-b_2(\sqrt{b_1^2 + 2(r+\lambda)} + b_1)} g\left(T, \sqrt{b_1^2 + 2(r+\lambda)}, -b_2\right) \\ &\quad + S_0 e^{-\left(\lambda + \frac{\sigma^2}{2}\right)T} V(\sigma, -d(T, K), T; -b_1, -b_2) \\ &\quad - K e^{-(r+\lambda)T} V(0, -d(T, K), T; -b_1, -b_2). \end{aligned} \quad (4.7)$$

If $L \in (D_1, D_2)$ and $T > \tau^*$, then the option price can be presented as

$$F = (L - K) e^{-b_2(\sqrt{b_1^2 + 2(r+\lambda)} + b_1)} g\left(T - \tau^*, \sqrt{b_1^2 + 2(r+\lambda)}, -b_2\right)$$

$$+ e^{-(r+\lambda)(T-\tau^*)} \int_{-\infty}^{-d(\tau^*, L)} A\left(S_0 e^{\left(r - \frac{\sigma^2}{2}\right)\tau^* + \sigma y}, \tau^*\right) f(\tau^*, y) dy. \quad (4.8)$$

Finally, if $L \geq D_2$ or $L \in (D_1, D_2) \cap T \leq \tau^*$, then the option turns to an ordinary American call.

Proof. The case when $L \geq D_2$ or $L \in (D_1, D_2)$ jointly with $\tau^* \geq T$ is obvious, since both exercise boundaries coincide, $c(t) \equiv c^A(t)$ for $t \leq T$.

Suppose now that $K < L \leq D_1$. Note that this is possible only when $r > 0$. Hence, the exercise boundary of the corresponding uncapped option is always above the cap and therefore the optimal boundary for the capped option is simply the value L . Let us notate by ζ the first hitting moment to the cap level L . If the asset starts below the cap, then the option price is

$$\begin{aligned} F &= E \left[e^{-(r+\lambda)\zeta} (L - K) I_{\zeta \leq T} \right] + E \left[e^{-(r+\lambda)T} (S_T - K)^+ I_{\zeta > T} \right] \\ &= (L - K) E \left[e^{-(r+\lambda)\zeta} I_{\zeta \leq T} \right] + S_0 e^{-\left(\lambda + \frac{\sigma^2}{2}\right)T} E \left[e^{\sigma B_T} I_{\zeta > T, S_T > K} \right] \\ &\quad - K e^{-(r+\lambda)T} E \left[I_{\zeta > T, S_T > K} \right]. \end{aligned} \quad (4.9)$$

It remains to use propositions Appendix A.1 and Appendix A.2 (Theorems 3.1 and 3.2 from Zaeviski [45]) to derive formula (4.7). Note that we do not need to use the opposite Brownian motion as we did in the put case. We use the arguments presented in Eq. (3.15) to prove formula (4.8). \square

Remark 4.1. Note that when $\lambda = 0$, the early exercising is never optimal for the uncapped option. It turns out that $D_1 = D_2 = \infty$ and therefore the first case of Theorem 4.2 holds.

We present below the analogue of the Corollary 3.1 for the perpetual capped call.

Corollary 4.1. When $T = \infty$, the early exercise boundary is the line $C = L \wedge D_2$. If the initial asset price is below it, $S_0 < C$, the option price is

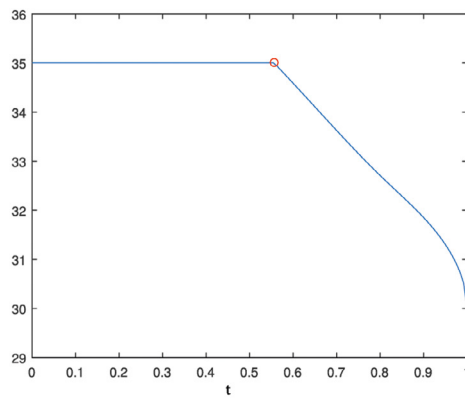
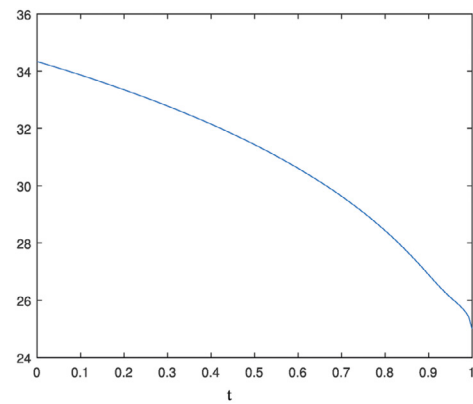
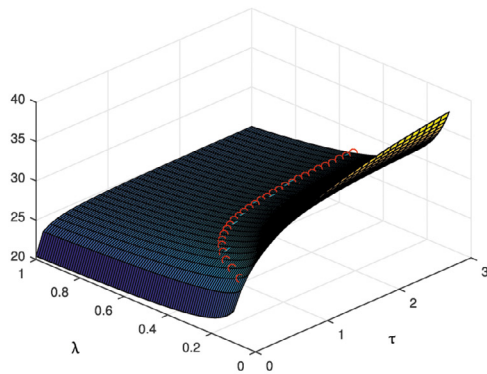
$$F = (c - K) \left(\frac{c}{x} \right)^{-\gamma}, \quad (4.10)$$

where γ is given by Eq. (4.1). If $S_0 \geq C$, then the option price is $F = S_0 - K$.

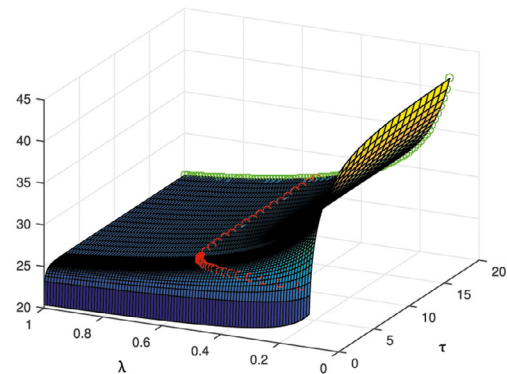
To implement Theorem 4.2 we can use a similar to the presented in Section 3.2 finite difference approach. The corresponding PDE turns to

$$\begin{aligned} F_t(t, x) + r x F_x(t, x) + \frac{1}{2} \sigma^2 x^2 F_{xx}(t, x) - r F(t, x) &= 0 \\ F(t, c^A(t)) &= \exp(-\lambda t) (c^A(t) - K), \quad t \in [0, T] \\ F(0, x) &= 0, \quad t \in [0, T] \\ F(T, x) &= \exp(-\lambda T) (x - K)^+, \quad 0 \leq x < c(T). \end{aligned} \quad (4.11)$$

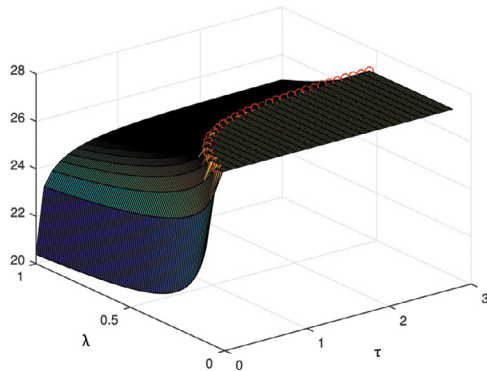
The equation is satisfied in the strip $(0, T) \times (0, c(t))$ and the boundary constraints are imposed on the lower, upper, and right boundaries. In the call case we do not need to use a Monte Carlo modification since the state space is closed at both sides. On the other hand if the strike or the exercise boundary are large the Monte Carlo modification can be very helpful. We have to change only the boundary constraints in the presented in Section 3.2 algorithm to obtain the prices of the American uncapped call options. Theorem 4.2 consists again from three parts – (A) the option can be an ordinary American call and thus it can be priced by the presented above Crank–Nicolson finite difference method, (B) the optimal boundary may coincide with the cap and hence the closed form formula is available, or (C) the capped option price can be given by Eq. (4.8) – in this case we can use the approach presented in Section 3.3 to evaluate numerically the integral.

(a) The optimal boundary, $\lambda = 0.04$.(b) The optimal boundary, $\lambda = 0.08$.

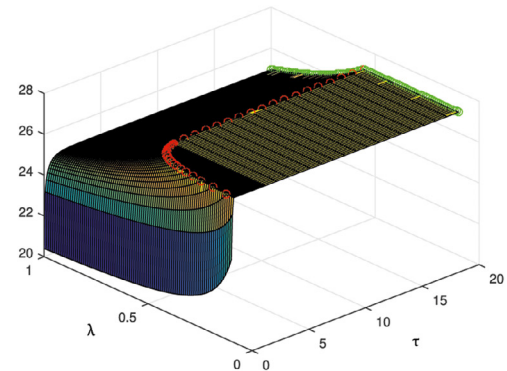
(c) The surface of the uncapped boundary – short maturities.



(d) The surface of the uncapped boundary – long maturities.



(e) The surface of the capped boundary – short maturities.



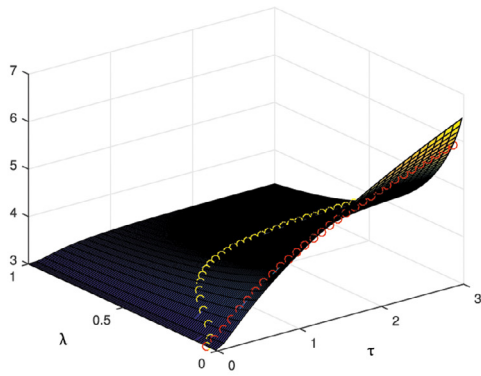
(f) The surface of the capped boundary – long maturities.

Fig. 3. Call capped options.

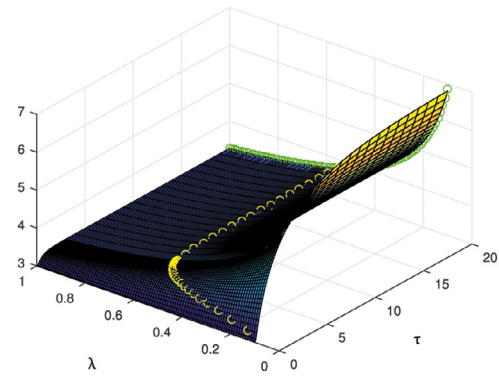
The typical forms of the early exercise boundary of the American capped call options can be seen in Fig. 3a and 3b. The used parameters are $r = 0.02$, $\sigma = 0.3$, $K = 20$, $T = 1$, and $L = 35$. At Fig. 3a we present the optimal boundary assuming that the additional discount factor is $\lambda = 0.04$. The initial value is $D_1 = 30$, whereas the perpetual one is $D_2 = 62.9719$. The critical value for the time to maturity is $\tau^* = 0.4437$ and it is marked by a red point. For Fig. 3b we use a value $\lambda = 0.08$, which leads to the corresponding ter-

minal levels $D_1 = 25$, $D_2 = 45.1842$, and $\tau^* = 1.1569$. Since $\tau^* > T$, the capped and uncapped options coincide.

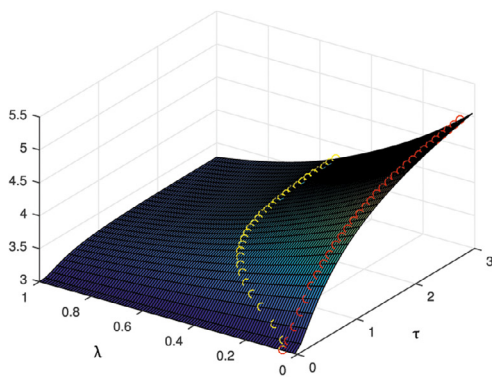
A reasonable hypothesis is that the speed of the convergence of the optimal boundary to the perpetual level is larger for the larger values of the discount factor λ . To confirm this we consider $\lambda \in (0.1, 1)$. The short maturity behavior – $\tau \in (0, 3)$ – for the uncapped and capped options is presented in Fig. 3c and 3d, respectively. We mark again by red points the values at which the



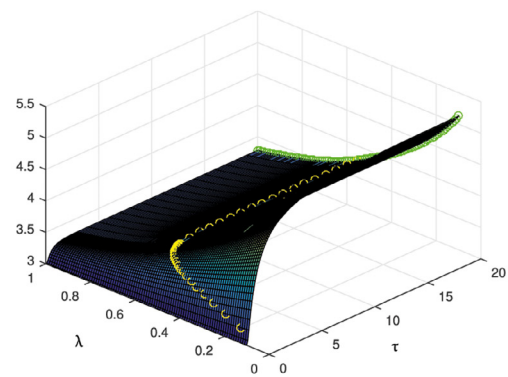
(a) Pure American call option prices, short maturities



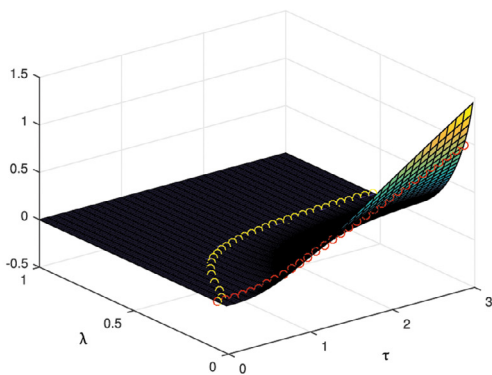
(b) Pure American call option prices, long maturities



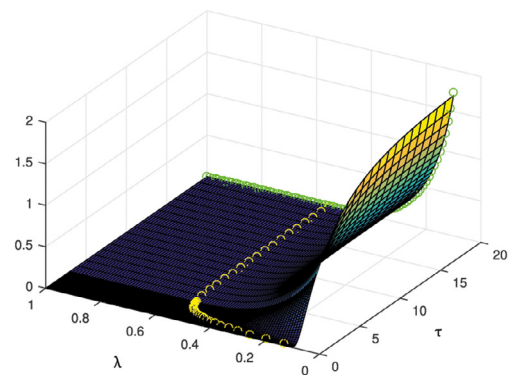
(c) American capped call option prices, short maturities



(d) American capped call option prices, long maturities



(e) Call premium, short maturities



(f) Call premium, long maturities

Fig. 4. Call option prices.

uncapped boundary rises above the cap L . At Fig. 3d and 3f we present the boundary surface for the longer maturities $\tau \in (0, 20)$. The perpetual values calculated by Corollary 4.1 are plotted by green points. We can see that the optimal boundaries are relatively close to them for $\tau = 20$. Hence, the boundaries really converge faster for the larger discount factors.

We present the behavior of the option prices at Fig. 4. The initial asset price is assumed to be $S_0 = 23$, whereas the cap level

is $L = 27$. Fig. 4a, 4c, and 4e illustrate the short time range – $\tau \in (0, 3)$. The discount factor is varied among $\lambda \in (0.01, 1)$. We again mark by red and yellow points the critical values λ_1 and λ_2 , respectively, at which the capped option changes its features. More precisely, if $\lambda \leq \lambda_1$, then the optimal boundary of the capped option coincides by the cap L . Hence its price is calculated through formula (4.7). We use formula (4.8) when $\lambda \in (\lambda_1, \lambda_2)$. If the discount factor is large enough, $\lambda \geq \lambda_2$, both options coincide. Note

Table 2
Call option prices.

$\lambda = 0$	American	$L = 21$	$L = 24$	$L = 27$	$L = 30$	$L = 33$
$\tau = 0.5$	1.7824	0.8070/1	1.6730/1	1.7692/1	1.7797/1	1.7817/1
$\tau = 1$	2.5643	0.8572/1	2.1342/1	2.4622/1	2.5351/1	2.5537/1
$\tau = 2$	3.7006	0.8928/1	2.5376/1	3.2320/1	3.5036/1	3.6097/1
$\tau = 3$	4.5886	0.9083/1	2.7320/1	3.6597/1	4.1130/1	4.3331/1
$\lambda = 0.02$	American	$L = 21$	$L = 24$	$L = 27$	$L = 30$	$L = 33$
$\tau = 0.5$	1.7644	0.8057/1	1.6640/1	1.7552/1	1.7633/1	1.7644/1
$\tau = 1$	2.5134	0.8551/1	2.1174/1	2.4323/1	2.4964/1	2.5095/1
$\tau = 2$	3.5577	0.8897/1	2.5084/1	3.1744/1	3.4229/1	3.5112/1
$\tau = 3$	4.3315	0.9045/1	2.6930/1	3.5787/1	3.9948/1	4.1841/1
$\lambda = 0.04$	American	$L = 21$	$L = 24$	$L = 27$	$L = 30$	$L = 33$
$\tau = 0.5$	1.7472	0.8044/1	1.6551/1	1.7413/1	1.7470/1	1.7472/2
$\tau = 1$	2.4666	0.8531/1	2.1008/1	2.4030/1	2.4584/1	2.4661/2
$\tau = 2$	3.4380	0.8867/1	2.4798/1	3.1183/1	3.3445/1	3.4157/2
$\tau = 3$	4.1287	0.9008/1	2.6551/1	3.5004/1	3.8810/1	4.0414/2
$\lambda = 0.06$	American	$L = 21$	$L = 24$	$L = 27$	$L = 30$	$L = 33$
$\tau = 0.5$	1.7310	0.8030/1	1.6463/1	1.7275/2	1.7310/2	1.7310/3
$\tau = 1$	2.4252	0.8511/1	2.0843/1	2.3739/2	2.4211/2	2.4252/2
$\tau = 2$	3.3350	0.8837/1	2.4518/1	3.0635/2	3.2684/2	3.3244/2
$\tau = 3$	3.9569	0.8971/1	2.6183/1	3.4246/2	3.7716/2	3.9055/2
$\lambda = 0.08$	American	$L = 21$	$L = 24$	$L = 27$	$L = 30$	$L = 33$
$\tau = 0.5$	1.7161	0.8017/1	1.6375/1	1.7139/2	1.7161/2	1.7161/3
$\tau = 1$	2.3874	0.8491/1	2.0681/1	2.3454/2	2.3853/2	2.3874/2
$\tau = 2$	3.2419	0.8808/1	2.4243/1	3.0101/2	3.1948/2	3.2376/2
$\tau = 3$	3.8044	0.8936/1	2.5825/1	3.3513/2	3.6666/2	3.7762/2
$\lambda = 0.1$	American	$L = 21$	$L = 24$	$L = 27$	$L = 30$	$L = 33$
$\tau = 0.5$	1.7021	0.8004/1	1.6288/1	1.7006/2	1.7021/2	1.7021/3
$\tau = 1$	2.3518	0.8471/1	2.0520/1	2.3175/2	2.3510/2	2.3518/2
$\tau = 2$	3.1562	0.8780/1	2.3974/1	2.9581/2	3.1237/2	3.1549/2
$\tau = 3$	3.6667	0.8901/1	2.5476/1	3.2805/2	3.5657/2	3.6530/2

that λ_1 is just the discount value which leads to $D_1 = L$, i.e.

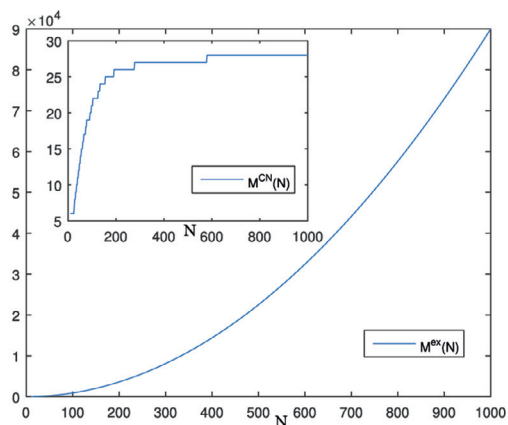
$$\lambda_1 = \frac{rK}{L - K}. \quad (4.12)$$

Our parameters lead to $\lambda_1 = 0.0571$. Let us mention again that if $\tau = 0$ then both critical values coincide – Fig. 4a, 4c, and 4e confirm this.

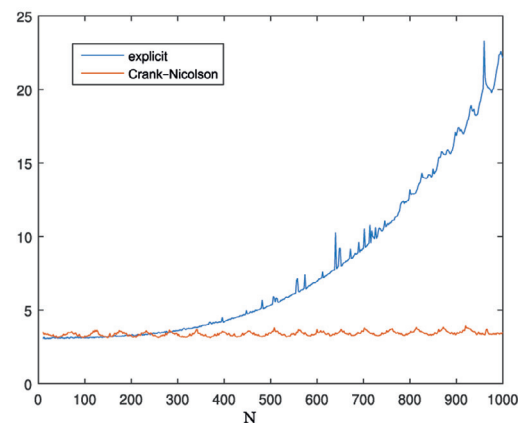
The Fig. 4b, 4d, and 4f presents the uncapped and capped prices and the corresponding premium for capping assuming that $\tau \in (0, 20)$. Differently for the short maturity case, we consider

discount factors larger than 0.1 – $\lambda \in (0.1, 1)$. In such a way we confirm again that for larger discount values the convergence to the perpetual levels is faster. They are calculated by the use of Corollary 4.1 and are marked by green. We do not show the first critical value for the discount factor since it is out of our interval, $\lambda_1 \equiv 0.0571 < 0.1$. The second critical values which exceed 0.1 are marked by yellow.

Some particular call option prices are presented in Table 2. We assume again that the option is at-the-money, i.e. $S_0 \equiv K = 20$. We vary the cap value among $L \in \{21, 24, 27, 30, 33\}$, the time



(a) The steps – $M^{ex}(N)$ and $M^{CN}(N)$



(b) Time in seconds

Fig. 5. Accuracy results.

to maturity among $\{0.5, 1, 2, 3\}$, and the discount rate among $\{0, 0.02, 0.04, 0.06, 0.08, 0.1\}$. Note that early exercising of an uncapped American option is never optimal prematurely when $\lambda = 0$. Thus it turns to a European one. Accordingly, we use the Black–Scholes formula to derive the prices presented in the first column of the first section of Table 2. Let us mention that the algorithm for call pricing do not involve a preliminary calculation of the option prices at the upper boundary. For this we use a very precise grid considering $M = 20\,000$ and $N = 5\,000$. Right to the corresponding option price we place the case of Theorem 4.2 which is actual.

Finally, we present one more numerical experiment related to the algorithm accuracy and the convergence speed. The reported results are performed by the use of MATLAB with Intel i7-10510U (4.9G)/ 16GB RAM/ 1000GB SSD. We compare the presented above Crank–Nicolson method with one in which the American option prices are calculated via the explicit finite difference approach adopted in Zaeviski [27]. The following parameters are used – $r = 0.02$, $\sigma = 0.03$, $\lambda = 0.04$, $K = 20$, $L = 33$, and $S_0 = 30$. As we mentioned above the algorithm with $M = 20\,000$ and $N = 5\,000$ steps produces results very closed to the real prices – 10.2518 and 10.3057 for the capped and uncapped options. We vary the number of the state steps for the explicit method between $N \in [10, 1\,000]$. We choose the number of the time steps $M^{ex}(N)$ as the lowest value satisfying the stability condition (3.19) which now turns to $\frac{m}{n^2} < \frac{1}{138.7326}$. Thus $M^{ex}(N)$ increases from 9 to 90 000. The highest value of N is chosen as 1 000 because it leads to the American price close to the real value 10.3057. For every value of N we obtain the lowest value of M – we denote it by $M^{CN}(N)$ – which makes the American option price produced by the Crank–Nicolson method better than the corresponding price derived trough the explicit algorithm. It turns out that only $M^{CN}(1000) = 28$ instead $M^{ex}(1000) = 90\,000$ steps are enough for the Crank–Nicolson method to produce a result very closed to the real option price. The same conclusion is true for the capped options too. All results are presented in Fig. 5a and 5b. The first one is for the time steps and the second one is for the corresponding times.

5. Conclusions

We have examined in this paper the discounted American capped options. The theorems for the form of the optimal regions have been obtained. It turns out that the early exercise boundary for the put/call capped option is the maximum/minimum between the boundary of the corresponding uncapped option and the cap value. The formulas for the option prices have been developed. There exist three possible cases – (A) the capped option price may coincide with the corresponding uncapped one, (B) the optimal boundary of the capped option may coincide with the cap value and thus the pricing problem turns to a first hitting problem, and (C) a mixture between the previous two cases. We have derived a closed form formula in case (B). We have presented a Crank–Nicolson finite difference approach for deriving the price of the American uncapped options. Using it we price the related capped option when cases (A) or (C) are actual. At last but not least this numerical method allows us to calculate jointly both of capped and uncapped option prices and the related premium for capping. This reduces significantly the computational time.

Declaration of Competing Interest

The authors declare that they have no known competing financial interests or personal relationships that could have appeared to influence the work reported in this paper.

CRedit authorship contribution statement

Tsvetelin S. Zaeviski: Conceptualization, Methodology, Formal analysis, Software, Investigation, Writing – original draft, Writing – review & editing.

Acknowledgments

This research has been partially supported by Grant No BG05M2OP001-1.001-0003, financed by the Science and Education for Smart Growth Operational Program (2014–2020) and co-financed by the European Union through the European structural and Investment funds and by the project KP-06-N32/8 with the Bulgarian National Science Fund.

Appendix A. Some propositions

Let $b(t) = b_1 t + b_2$ be a linear function starting at a positive point, $b_2 > 0$. The following propositions hold.

Proposition A.1. We have for $\theta > 0$

$$L(T, \theta; b_1, b_2) = E[e^{-\theta \tau} I_{\tau \leq T}] = e^{b_2(\sqrt{b_1^2 + 2\theta} - b_1)} g\left(T; \sqrt{b_1^2 + 2\theta}, b_2\right), \quad (\text{A.1})$$

where the function $g(\cdot)$ is given in Eq. (3.13).

Proof. The proposition is proven as Theorem 3.1 from Zaeviski [45]. \square

Proposition A.2. For all z such that $z < b(T)$ the following statement holds

$$E[e^{\theta B_T} I_{B_T > z, \tau > T}] = V(\theta, z, T; b_1, b_2), \quad (\text{A.2})$$

where the function $V(\cdot)$ is given again in Eq. (3.13).

Proof. The proposition is proven as Theorem 3.2 from Zaeviski [45]. \square

Proposition A.3. For all z and t such that $z < b(t)$ the following statement holds

$$P(B_t < y, \tau > t) = \int_{-\infty}^y f(t, u) du, \quad (\text{A.3})$$

where the function $f(\cdot)$ is given in Eq. (3.14).

Proof. This statement can be found as Eq. (3.7) from Zaeviski [45]. \square

References

- [1] Brennan MJ, Schwartz ES. The valuation of American put options. *J Financ* 1977;32(2):449–62.
- [2] Myneni R. The pricing of the American option. *Ann Appl Probab* 1992;2(1):1–23. doi:10.1214/aoap/1177005768.
- [3] Karatzas I. On the pricing of American options. *Appl Math Optim* 1988;17(1):37–60.
- [4] Jaillet P, Lamberton D, Lapeyre B. Variational inequalities and the pricing of American options. *Acta Appl Math* 1990;21(3):263–89.
- [5] Rogers L. Monte Carlo valuation of American options. *Math Financ* 2002;12(3):271–86.
- [6] Nunes J, Dias J, JP R. The early exercise boundary under the jump to default extended CEV model. *Appl Math Optim* 2018;1–31.
- [7] Chen C, Wang Z, Yang Y. A new operator splitting method for American options under fractional Black–Scholes models. *Comput Math Appl* 2019;77(8):2130–44. doi:10.1016/j.camwa.2018.12.007.
- [8] Chan T. Hedging and pricing early-exercise options with complex Fourier series expansion. *N Am J Econ Financ* 2019. doi:10.1016/j.najef.2019.04.016.
- [9] Chan T. An SFP-FCC method for pricing and hedging early-exercise options under Lévy processes. *Quant Financ* 2020;20(8):1325–43. doi:10.1080/14697688.2020.1736322.
- [10] Deng G. Pricing American put option on zero-coupon bond in a jump-extended CIR model. *Commun Nonlinear Sci Numer Simul* 2015;22(1):186–96. doi:10.1016/j.cnsns.2014.10.003.

- [11] Haghi M, Mollapourasl R, Vanmaele M. An RBF-FD method for pricing American options under jump-diffusion models. *Comput Math Appl* 2018;76(10):2434–59. doi:[10.1016/j.camwa.2018.08.040](https://doi.org/10.1016/j.camwa.2018.08.040).
- [12] Gan X, Yang Y, Zhang K. A robust numerical method for pricing American options under Kou's jump-diffusion models based on penalty method. *J Appl Math Comput* 2020;62(1):1–21.
- [13] Boen L, in 't Hout KJ. Operator splitting schemes for American options under the two-asset Merton jump-diffusion model. *Appl Numer Math* 2020;153:114–31. doi:[10.1016/j.apnum.2020.02.004](https://doi.org/10.1016/j.apnum.2020.02.004).
- [14] Jeon J, Huh J, Park K. An analytic approximation for valuation of the American option under the Heston model in two regimes. *Comput Econ* 2020;56:499–528. doi:[10.1007/s10614-019-09939-2](https://doi.org/10.1007/s10614-019-09939-2).
- [15] Mehrdoust F, Noorani I, Hamdi A. Calibration of the double Heston model and an analytical formula in pricing American put option. *J Comput Appl Math* 2021;113422. doi:[10.1016/j.cam.2021.113422](https://doi.org/10.1016/j.cam.2021.113422).
- [16] Arregui I, Salvador B, Ševčovič D, Vázquez C. PDE models for American options with counterparty risk and two stochastic factors: mathematical analysis and numerical solution. *Comput Math Appl* 2020;79(5):1525–42. doi:[10.1016/j.camwa.2019.09.014](https://doi.org/10.1016/j.camwa.2019.09.014).
- [17] Deng G. American continuous-installment options of barrier type. *J Syst Sci Complex* 2014;27(5):928–49.
- [18] Park K, Jeon J. A simple and fast method for valuing American knock-out options with rebates. *Chaos Solitons Fractals* 2017;103:364–70.
- [19] Nunes J, Ruas J, Dias J. Early exercise boundaries for American-style knock-out options. *Eur J Oper Res* 2020;285(2):753–66. doi:[10.1016/j.ejor.2020.02.006](https://doi.org/10.1016/j.ejor.2020.02.006).
- [20] Michael F. Black-Scholes like closed form formulas and numerical solutions for American style options. *Phys A Stat Mech Appl* 2020;550:124379. doi:[10.1016/j.physa.2020.124379](https://doi.org/10.1016/j.physa.2020.124379).
- [21] Deng G. Pricing perpetual American floating strike lookback option under multiscale stochastic volatility model. *Chaos Solitons Fractals* 2020;141:110411.
- [22] Woo M, Choe G. Pricing of American lookback spread options. *Stoch Process Their Appl* 2020;130(10):6300–18. doi:[10.1016/j.spa.2020.05.012](https://doi.org/10.1016/j.spa.2020.05.012).
- [23] Zhang X, Li L, Zhang G. Pricing American drawdown options under Markov models. *Eur J Oper Res* 2021. doi:[10.1016/j.ejor.2021.01.033](https://doi.org/10.1016/j.ejor.2021.01.033).
- [24] Soleymani F, Barfeie M, Haghani F. Inverse multi-quadric RBF for computing the weights of FD method: application to American options. *Commun Nonlinear Sci Numer Simul* 2018;64:74–88.
- [25] Cen Z, Chen W. A HODIE finite difference scheme for pricing American options. *Adv Differ Equ* 2019;2019(1):1–17.
- [26] Krzyżanowski G, Magdziarz M. A computational weighted finite difference method for American and barrier options in subdiffusive Black-Scholes model. *Commun Nonlinear Sci Numer Simul* 2021;96:105676. doi:[10.1016/j.cnsns.2020.105676](https://doi.org/10.1016/j.cnsns.2020.105676).
- [27] Zaeviski T. A new approach for pricing discounted American options. *Commun Nonlinear Sci Numer Simul* 2021;97:105752. doi:[10.1016/j.cnsns.2021.105752](https://doi.org/10.1016/j.cnsns.2021.105752).
- [28] Kifer Y. Game options. *Financ Stoch* 2000;4(4):443–63. doi:[10.1007/PL00013527](https://doi.org/10.1007/PL00013527).
- [29] Kifer Y. Dynkin's games and Israeli options. *ISRN Probab Stat* 2013;2013.
- [30] Zaeviski T. Discounted perpetual game call options. *Chaos Solitons Fractals* 2020;131:109503. doi:[10.1016/j.chaos.2019.109503](https://doi.org/10.1016/j.chaos.2019.109503).
- [31] Zaeviski T. Discounted perpetual game put options. *Chaos Solitons Fractals* 2020;137:109858. doi:[10.1016/j.chaos.2020.109858](https://doi.org/10.1016/j.chaos.2020.109858).
- [32] Zaeviski T. Perpetual game options with a multiplied penalty. *Commun Nonlinear Sci Numer Simul* 2020;85:105248. doi:[10.1016/j.cnsns.2020.105248](https://doi.org/10.1016/j.cnsns.2020.105248).
- [33] Broadie M, Detemple J. American capped call options on dividend-paying assets. *Rev Financ Stud* 1995;8(1):161–91.
- [34] Detemple J, Tian W. The valuation of American options for a class of diffusion processes. *Manag Sci* 2002;48(7):917–37.
- [35] Broadie M, Detemple J. American option valuation: new bounds, approximations, and a comparison of existing methods. *Rev Financ Stud* 1996;9(4):1211–50.
- [36] Deng D, Peng C. New methods with capped options for pricing American options. *J Appl Math* 2014;2014.
- [37] Heston S. A closed-form solution for options with stochastic volatility with applications to bond and currency options. *Rev Financ Stud* 1993;6(2):327–43.
- [38] He X-J, Lin S. An analytical approximation formula for barrier option prices under the Heston model. *Comput Econ* 2021;1–13.
- [39] Bates D. Jumps and stochastic volatility: the exchange rate processes implicit in Deutschmark options. *Rev Financ Stud* 1996;9:69–107.
- [40] Zaeviski TS, Kim YS, Fabozzi FJ. Option pricing under stochastic volatility and tempered stable Lévy jumps. *Int Rev Financ Anal* 2014;31:101–8. doi:[10.1016/j.irfa.2013.10.004](https://doi.org/10.1016/j.irfa.2013.10.004).
- [41] He X-J, Lin S. A fractional Black-Scholes model with stochastic volatility and European option pricing. *Expert Syst Appl* 2021;178:114983.
- [42] He X-J, Chen W. Pricing foreign exchange options under a hybrid Heston-Cox-Ingersoll-Ross model with regime switching. *IMA J Manag Math* 2021;33(2):255–72. doi:[10.1093/imaman/dpab013](https://doi.org/10.1093/imaman/dpab013).
- [43] He X-J, Chen W. A closed-form pricing formula for European options under a new stochastic volatility model with a stochastic long-term mean. *Math Financ Econ* 2021;15(2):381–96.
- [44] Crank J, Nicolson P. A practical method for numerical evaluation of solutions of partial differential equations of the heat-conduction type. *Math Proc Camb Philos Soc* 1947;43(1):50–67.
- [45] Zaeviski T. Laplace transforms for the first hitting time of a Brownian motion. *C. R. Acad. Bulg. Sci.* 2020;73(7):934–41. doi:[10.7546/CRABS.2020.07.05](https://doi.org/10.7546/CRABS.2020.07.05).